

# Development of an Evaluation System for the Flow Rate Characteristics of a Supply Unit in a Powered Air-Purifying Respirator: Dependency on Differential Pressure, Voltage, and PWM Duty Value

Yusaku Fujii<sup>1, a, \*</sup>, Akihiro Takita<sup>1, b</sup>, Seiji Hashimoto<sup>1, c</sup>, Noriaki Yoshiura<sup>2, d</sup>, Takao Yamaguchi<sup>1, e</sup>, Kenji Amagai<sup>1, f</sup>, Chihiro Kamio<sup>1, g</sup>, Edwin Carcasona<sup>3, h</sup> and Ronald M Galindo<sup>4, i</sup>

<sup>1</sup>School of Science and Technology, Gunma University, Kiryu, Japan

<sup>2</sup> Department of Information and Computer Sciences, Saitama University, Saitama, Japan

<sup>3</sup> Faculty of Engineering, University of San Carlos, Cebu, Philippines

<sup>4</sup> Faculty of Engineering, Cebu Technological University, Cebu, Philippines

\*Corresponding author

<sup>a</sup><fujii@gunma-u.ac.jp>, <sup>b</sup><takita@gunma-u.ac.jp>, <sup>c</sup><hashimotos@gunma-u.ac.jp>, <sup>d</sup><yoshiura@fmx.ics.saitama-u.ac.jp>, <sup>e</sup><yamagme3@gunma-u.ac.jp>, <sup>f</sup><amagai@gunma-u.ac.jp>, <sup>g</sup><chihiro.kamio@gunma-u.ac.jp>, <sup>h</sup><edcarc123055@yahoo.com>, <sup>i</sup><ronald.galindo@ctu.edu.ph>

**Keywords:** Powered Air-Purifying Respirator (PAPR), Flow rate modeling, Differential pressure, PWM duty control, Respiratory simulation, Positive pressure hood, Airborne infection control, Flow estimation algorithm, Smart respiratory device.

**Abstract.** As a sustainable alternative to strict behavioral restrictions (lockdowns) during pandemics, the authors have been developing a low-cost, high-performance Powered Air-Purifying Respirator (PAPR) for public use. A PAPR supplies filtered air into a hood under positive pressure, thereby preventing the intrusion of external aerosols. To achieve both high protective performance and wearing comfort, it is essential to precisely understand and model the operating characteristics of the supply unit—specifically, how the airflow rate responds to differential pressure ( $\Delta P$ ), applied voltage ( $V$ ), and the duty value ( $n$ ) of PWM control.

In this study, the authors developed a dedicated evaluation system equipped with a pressure buffer that simulates the PAPR hood environment and a respiratory airflow simulator based on a piston-cylinder mechanism. Using this system, a multivariate polynomial regression model  $Q_e(\Delta P, n)$  was derived to express the supply flow rate  $Q_1$  as a function of  $\Delta P$  and  $n$ . To validate the model, the estimated supply flow rate  $Q_e$  was subtracted from the measured exhaust flow rate  $Q_2$  to obtain an estimated respiratory flow, which was then compared with the independently measured simulated respiratory flow  $Q_3$ . The results demonstrated temporal and quantitative agreement between the two, confirming that noninvasive, real-time estimation of respiratory states, including inhalation/exhalation transitions, is feasible.

The proposed evaluation system and regression model are promising not only for static performance testing of supply units but also as foundational tools for developing breathing-synchronized assistive control and enhancing the overall intelligence and comfort of PAPRs.

## 1. Introduction

The COVID-19 pandemic [1-3] has had a profound impact on global society and the economy. Future crises of a similar nature are likely to recur due to the emergence of new variants and airborne infectious diseases [4,5]. To mitigate the spread of such infections, fundamental measures such as

mask-wearing, ventilation, and vaccination have been implemented. However, in emergency situations, stricter interventions such as lockdowns are often enforced [6]. Lockdowns, while effective in infection control, impose significant burdens on daily life and economic activity, raising concerns about their sustainability. Therefore, the development of realistic and effective alternatives to lockdowns is an urgent issue.

The authors have focused on the potential of the Powered Air-Purifying Respirator (PAPR) as a promising alternative for public use [7]. PAPRs deliver filtered air into a hood using a fan and maintain a positive pressure inside the hood to prevent the intrusion of airborne aerosols. This mechanism, originally designed for healthcare professionals, offers high levels of respiratory protection [8,9]. In particular, HEPA filters provide exceptional filtration performance, and the positive pressure prevents external air infiltration, offering significantly better protection compared to N95 or surgical masks.

The authors have been developing a low-cost PAPR that retains the essential protective functions of medical-grade PAPRs while being suitable for use by the general public [7,10-12]. If proven effective, such a PAPR could serve as a practical strategy to suppress infection spread in future airborne pandemics without resorting to lockdowns, allowing people to maintain their daily lives. In this context, not only protective performance but also wearing comfort becomes a critical factor for public adoption.

One promising approach to improving comfort is real-time pressure control synchronized with respiratory activity [7,10]. For example, increasing the positive pressure during inhalation and facilitating exhaust during exhalation could reduce the wearer's breathing load. To implement such advanced control, it is essential to quantitatively understand the behavior of the supply unit - specifically, how the airflow rate responds to differential pressure ( $\Delta P$ ), supply voltage ( $V$ ), and PWM duty value ( $n$ ). This requires an experimental setup that can accurately evaluate the flow characteristics of the supply unit in isolation and a flow rate model based on those measurements [13].

In this study, the authors developed a new experimental system to evaluate how the supply airflow rate in a PAPR changes in response to differential pressure, voltage, and PWM duty value. Under steady-state conditions with the respiratory airflow simulator inactive, the supply flow rate  $Q_1$  was assumed to be equal to the measured exhaust flow rate  $Q_2 = Q_{2a} + Q_{2b}$ , allowing the modeling of  $Q_1$  as a function of  $\Delta P$ ,  $V$ , and  $n$ .

The following sections describe the structure and measurement method of the evaluation system (Figures 1-3), present the measured flow characteristics (Figure 4), and examine the validity and applicability of the resulting regression model by comparing it with experimental results under simulated respiratory conditions (Figure 5). This study contributes to establishing a foundational evaluation methodology for advancing the development of next-generation PAPRs for the general public.

## 2. Development of the Evaluation System

The evaluation system developed in this study, as shown in Figures 1 through 3, was designed to quantitatively assess the flow rate characteristics of the supply unit used in a Powered Air-Purifying Respirator (PAPR) for general public use. The system consists of a pressure buffer, a supply unit (blower and filter), an exhaust unit, and a respiratory airflow simulator. This configuration enables the simulation of both the positive-pressure environment inside a PAPR hood and the associated respiratory behavior.

The pressure buffer is composed of an acrylic container that provides a stable internal volume against pressure fluctuations. By connecting the outlets of the supply and exhaust systems to this buffer, it is possible to recreate internal pressure variations within a controlled space. The respiratory airflow simulator, constructed from an acrylic cylinder and piston, is designed to manually generate reciprocating flow that mimics human respiration (Figure 1).

The supply unit incorporates a blower (model: 9CRH0412P5J001, manufacturer: Sanyo Denki, rated voltage: 12 V, rated current: 2.52 A, maximum flow rate: 930 L/min, maximum static pressure: 1700 Pa) capable of PWM control. The unit operates at a supply voltage ranging from 6.0 to 12.0 V,

and the PWM duty value can be set between 0 and 255. This enables continuous control of the fan speed and corresponding supply flow rate. In this study, the PWM signal was directly input via a dedicated control line. A commercially available HEPA filter was mounted at the supply outlet to simulate high-efficiency particulate filtration required for airborne infection protection.

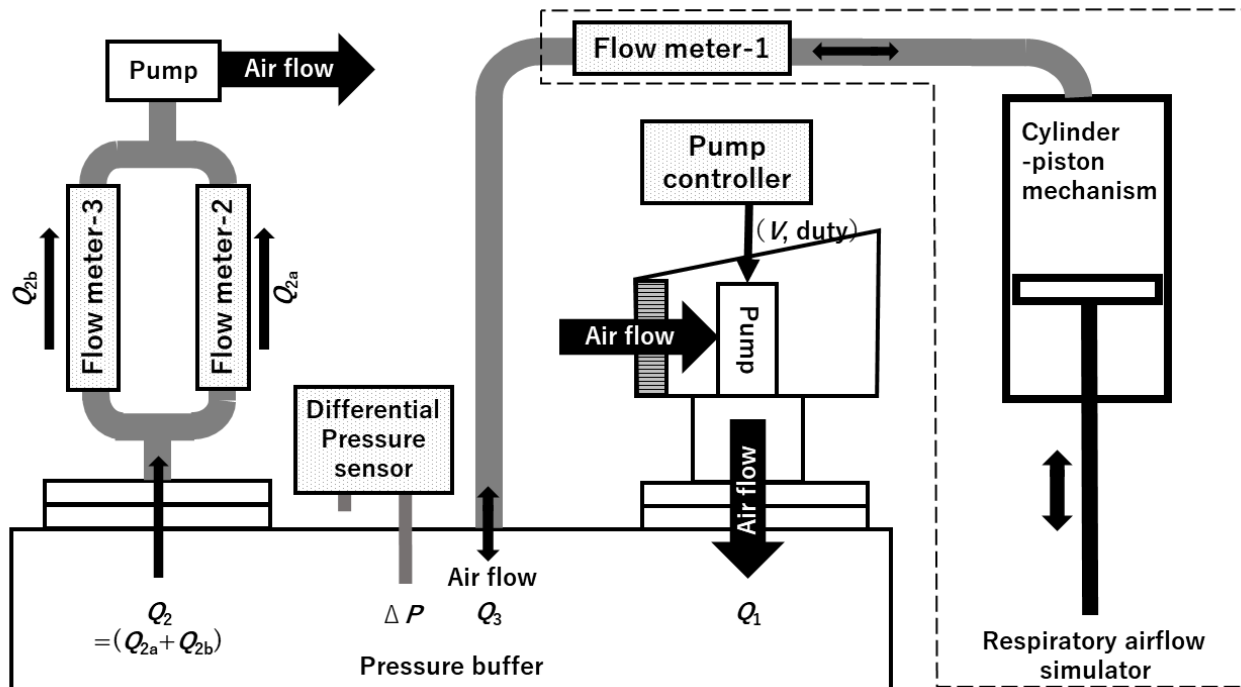


Figure 1. Schematic diagram of the evaluation system for supply unit flow characteristics.

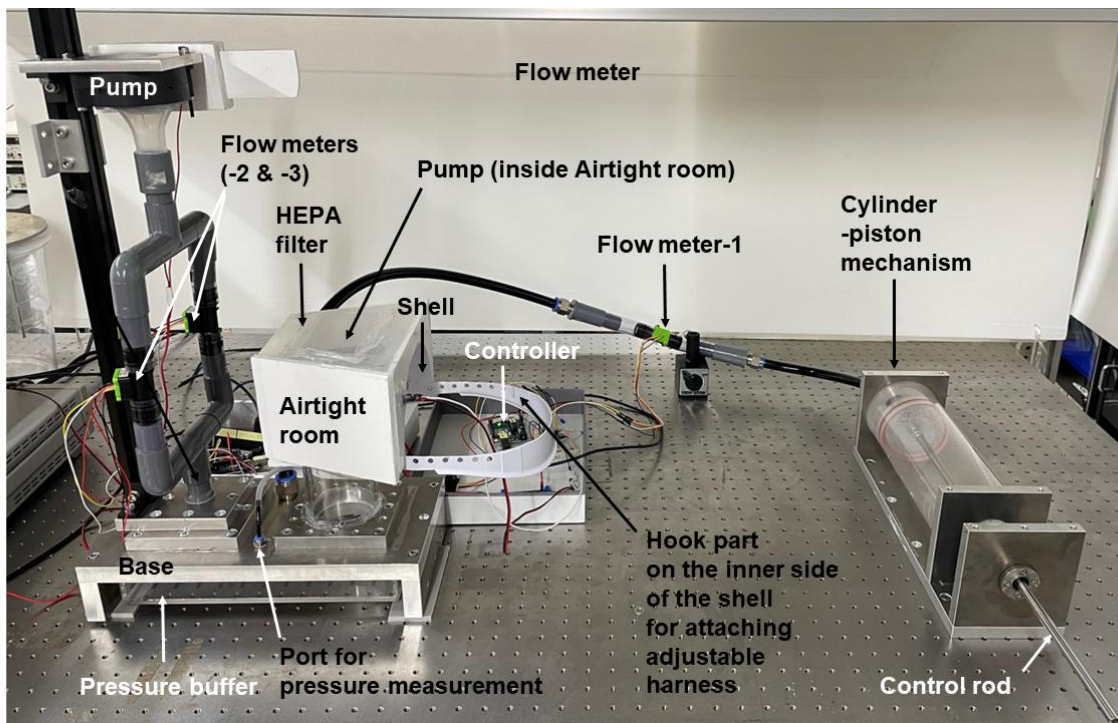


Figure 2. Photograph of the evaluation system for supply unit flow characteristics.

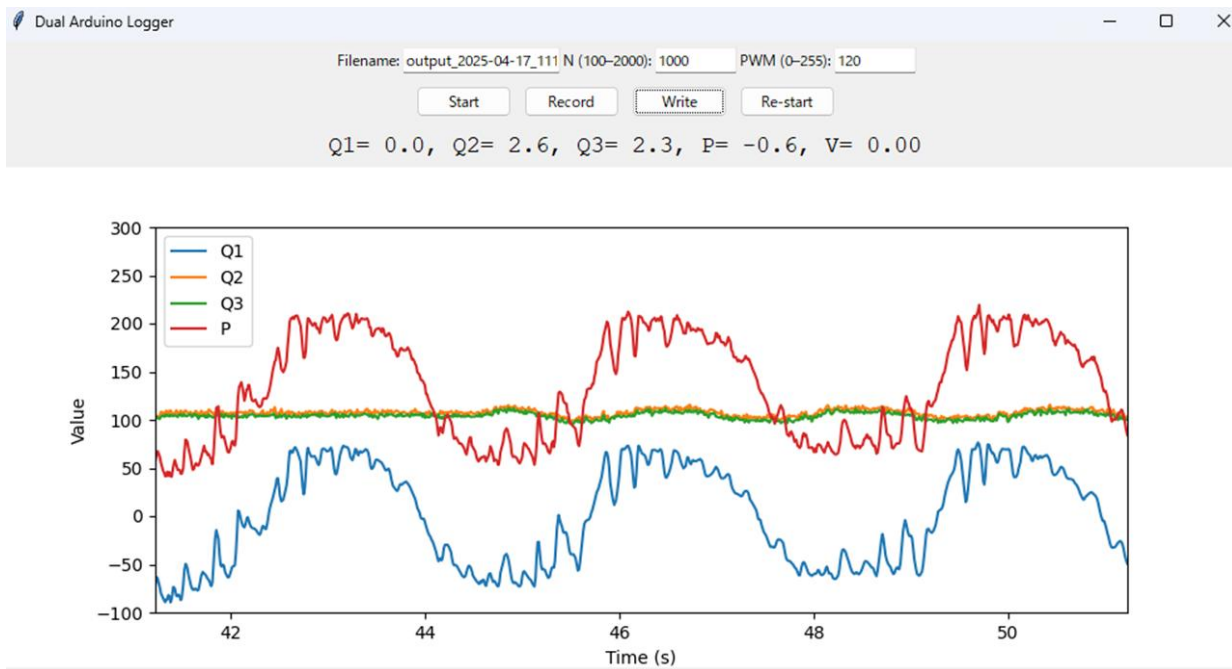


Figure 3. Screenshot of the Python application for real-time data acquisition and visualization.

On the exhaust side, air delivered by the supply unit is expelled from the pressure buffer through an exhaust fan and two parallel flow sensors (model: SFM3000-200-C, manufacturer: Sensirion; measurement range:  $\pm 200$  L/min, accuracy: 1.5%, response time: 0.5 ms, communication interface: I<sup>2</sup>C), as shown in Figure 2. This dual-sensor configuration was adopted to accommodate flow rates exceeding the rating of a single sensor. The exhaust flow rate  $Q_2$  is thus obtained as the sum of the readings from both sensors:  $Q_2 = Q_{2a} + Q_{2b}$ .

Meanwhile, the simulated respiratory flow  $Q_3$  introduced by the airflow simulator is independently measured by another flow sensor (Flow Meter-1). The differential pressure  $\Delta P$  within the pressure buffer is monitored with high accuracy using a differential pressure sensor (model: SDP810-500Pa, manufacturer: Sensirion; measurement range:  $\pm 500$  Pa, accuracy: 3%, communication interface: I<sup>2</sup>C). These sensors are connected to two Arduino Uno R3 microcontrollers via I<sup>2</sup>C communication. Arduino No.1 is responsible for measuring  $Q_3$ ,  $\Delta P$ , PWM duty value  $n$ , and fan voltage  $V$ , while Arduino No.2 handles measurements of  $Q_{2a}$  and  $Q_{2b}$ . Both microcontrollers transmit data to a PC via USB serial communication at 10 ms intervals.

The sensor outputs and control signals are centrally managed using a custom Python-based GUI application on a Windows PC (Figure 3). The application continuously receives data from both Arduinos and visualizes flow rates ( $Q_1$ ,  $Q_2$ ,  $Q_3$ ), differential pressure  $\Delta P$ , fan voltage  $V$ , and PWM duty value  $n$  in real time. The “Record” button allows acquisition and freezing of  $N$  continuous data points, from which mean values and standard deviations are calculated and displayed. Pressing the “Write” button appends a new line of data to a CSV file, including the timestamp and all calculated statistics such as  $Q_{1m}$ ,  $Q_{2m}$ ,  $Q_{3m}$ ,  $P_m$ ,  $V_m$ , and their corresponding standard deviations.

In the next section, this evaluation system will be used to investigate the static characteristics of the supply unit. The applied voltage  $V$  and PWM duty value  $n$  will be fixed, while the exhaust fan output is adjusted to vary the internal differential pressure  $\Delta P$ . Under these steady-state conditions (with the airflow simulator inactive), measurements will be performed in a state where the supply and exhaust flow rates are equal ( $Q_1 = Q_2$ ). From this dataset, a regression model expressing  $Q_1$  as a function of  $\Delta P$ ,  $V$ , and  $n$  will be constructed for use in subsequent control applications.

### 3. Evaluation of the Flow Characteristics of the Supply Unit

This section reports the results of quantitatively evaluating the flow characteristics of the supply unit using the experimental setup described in the previous section. First, under static conditions with the respiratory airflow simulator inactive, the supply voltage  $V$  and PWM duty value  $n$  were fixed, and the output of the exhaust fan was adjusted to control the differential pressure  $\Delta P$  inside the pressure buffer. A steady-state condition was thereby established in which the supply flow rate  $Q_1$  was equal to the exhaust flow rate  $Q_2$  (where  $Q_2 = Q_{2a} + Q_{2b}$ ). Using the measurement data obtained under this steady state, a regression model was constructed to express  $Q_1$  as a function of  $\Delta P$  and  $n$ .

Subsequently, the predictive accuracy of the derived regression model was evaluated under dynamic conditions, in which the respiratory airflow simulator was activated to introduce a simulated respiratory flow  $Q_3$ . The validity of the model was assessed by comparing the estimated and measured values of the respiratory flow under these conditions.

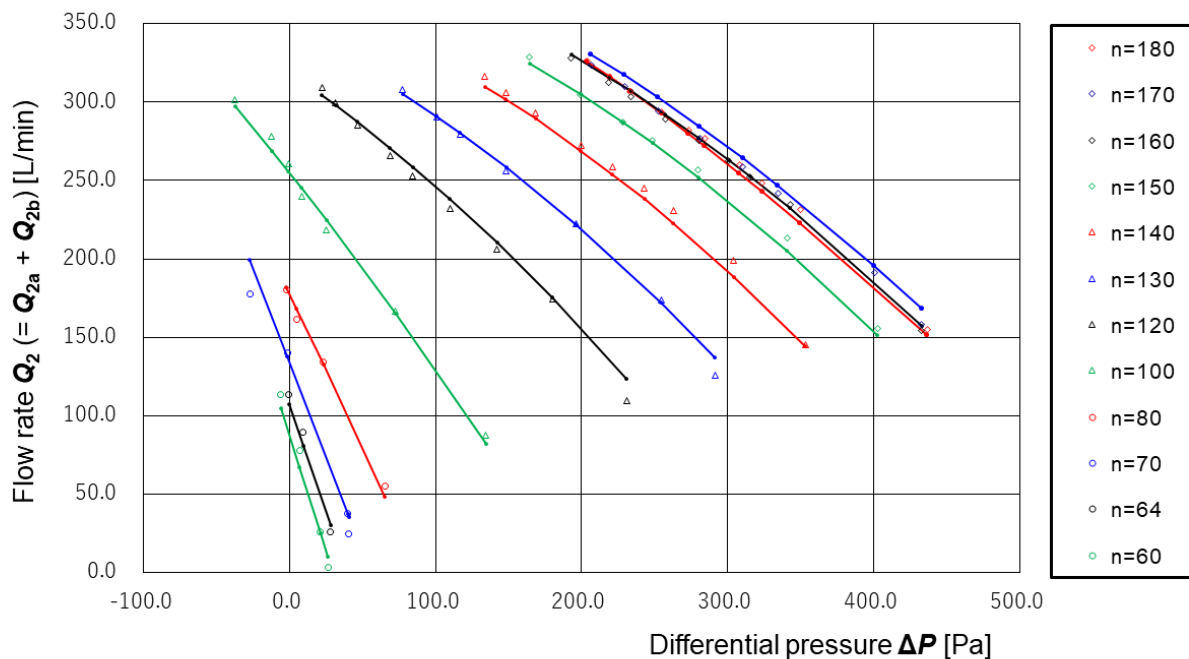


Figure 4. Measured flow rate characteristics of the supply unit as functions of differential pressure ( $\Delta P$ ) and PWM duty value ( $V = 6.0$  [V]).

#### 3.1 Regression Model of the Supply Flow Rate under Static Conditions

In this subsection, the flow characteristics of the supply unit under static conditions were formulated using a regression model, with the differential pressure  $\Delta P$  and PWM duty value  $n$  as independent variables. The pump used in this experiment was a high-output model, and under rated operation, it generated an excessively high flow rate. Therefore, in this study, the supply voltage was set to 6.0 V to allow for low-output operation.

The PWM duty value  $n$  was varied across 12 discrete levels:

$n = 180, 170, 160, 150, 140, 130, 120, 100, 80, 70, 64,$  and  $60$ .

For each setting, the output of the exhaust fan was adjusted to vary the differential pressure  $\Delta P$  over as wide a range as possible. The measurement time was set to 1 second ( $N = 100$ ), and the average value over this period was recorded as the representative value. The measurement results are presented in Figure 4.

In Figure 4, the horizontal axis represents the differential pressure  $\Delta P$  [Pa], and the vertical axis represents the supply flow rate  $Q$  [L/min]. The plot shows measurement points for each duty setting and the fitted regression curves (solid lines).

The regression model adopted the same polynomial form as that proposed by the authors in a previous study, expressed as a second-order polynomial with two variables ( $\Delta P$  and  $n$ ) and a total of nine terms:

$$Q_2 = Q_{2a} + Q_{2b} =$$

$$Q_e(\Delta P, n) = (1.110E-07)\Delta P^2 n^2 + (-2.886E-04)\Delta P n^2 + (-1.634E-02) n^2$$

$$+ (-2.686E-05)\Delta P^2 n + (9.022E-02)\Delta P n + (6.798E+00) n$$

$$+ (7.202E-04)\Delta P^2 + (-7.306E+00)\Delta P + (-2.617E+02)$$

Since the output of this pump appeared to remain constant at duty values of  $n = 180$  and above, the regression analysis was limited to the 12 levels between  $n = 60$  and 180. However, the outputs at  $n = 160, 170,$  and  $180$  were almost identical within the range of variation. This suggests that, for  $n$  values between 160 and 255, the pump maintains a constant output due to internal software-based output limitation.

From Fig. 4, it can be observed that within the range of  $n = 60$  to 160, the flow rate increases with rising duty values, and the relationship with  $\Delta P$  is nonlinear. It should be noted that this regression equation was derived under static conditions; therefore, in the following section, its validity under dynamic conditions will be examined.

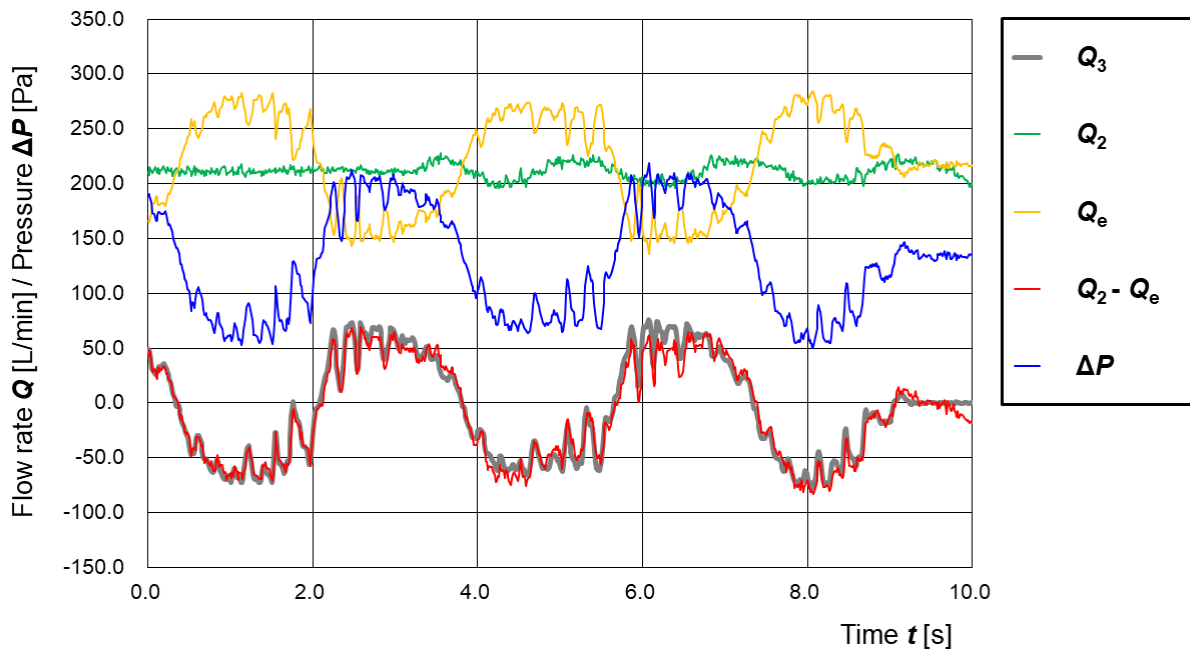


Figure 5. Time-series comparison of flow rates and differential pressure during simulated respiratory operation, including flow rate estimation results using the regression model.

### 3.2 Evaluation of the Performance of the Regression Model

In this subsection, the predictive accuracy of the regression model  $Q_1(\Delta P, n)$  was evaluated under dynamic conditions. The respiratory airflow simulator was activated to introduce reciprocating flow simulating inhalation and exhalation into the pressure buffer. During this test, the PWM duty value  $n$  and the supply voltage  $V$  were held constant ( $n = 120, V = 6.0$  [V]), and the output of the exhaust fan was adjusted to maintain the differential pressure  $\Delta P$  at approximately 120 Pa. Under these conditions, the respiratory simulator was manually operated to generate the simulated respiratory flow  $Q_3$ .

The measured values of  $\Delta P$  and the PWM duty value  $\mathbf{n}$  were substituted into the regression model  $Q_e(\Delta P, \mathbf{n})$  to estimate the supply flow rate. The difference between this estimated value and the measured exhaust flow rate  $Q_2 (= Q_{2a} + Q_{2b})$  was calculated as an estimated respiratory flow  $Q_2 - Q_e(\Delta P, \mathbf{n})$ . This approach enabled an indirect validation of the regression model's accuracy under dynamic conditions. All data were recorded continuously for 10 seconds at 10 ms intervals and plotted as time-series data in Figure 5.

Figure 5 shows the time variation of the following five data series:

- **Thick gray line:** measured simulated respiratory flow  $Q_3$
- **Green line:** measured exhaust flow rate  $Q_2 (= Q_{2a} + Q_{2b})$
- **Yellow line:** estimated supply flow rate  $Q_e(\Delta P, \mathbf{n})$  based on the regression model
- **Red line:** estimated respiratory flow  $Q_2 - Q_e(\Delta P, \mathbf{n})$
- **Blue line:** differential pressure  $\Delta P$  inside the pressure buffer

The results show that the estimated respiratory flow  $Q_2 - Q_e(\Delta P, \mathbf{n})$  agrees well with the actual respiratory flow  $Q_3$  in both temporal profile and magnitude. In particular, the timing of the transition between inhalation and exhalation (i.e., the point of sign inversion) matched closely between the estimated and measured values.

Additionally, all of the waveforms for  $Q_3$ ,  $Q_e(\Delta P, \mathbf{n})$ ,  $Q_2 - Q_e(\Delta P, \mathbf{n})$ , and  $\Delta P$  in the figure show periodic fine fluctuations superimposed on the broader respiratory cycle. These fluctuations are considered to reflect mechanical irregularities caused by the piston-cylinder-type respiratory simulator, such as backlash during manual operation and frictional variation depending on the piston's position. These mechanical factors are presumed to have generated small oscillations that appeared as similar patterns across the measured signals.

These findings confirm that the regression model  $Q_e(\Delta P, \mathbf{n})$ , developed under static conditions, remains valid under dynamic conditions involving respiratory motion. This result demonstrates the feasibility of real-time, noninvasive estimation of respiratory states (inhalation/exhalation) based on differential pressure and control signals, with promising applications in enhancing the comfort and assistive control functionality [14,15] of PAPRs.

This chapter confirms that the flow rate of the supply unit can be modeled as a function of differential pressure  $\Delta P$  and PWM duty value  $\mathbf{n}$ , and that the regression model remains effective even under dynamic conditions involving simulated respiratory behavior. In the next chapter, we discuss the potential for real-time control and respiratory state estimation using this model, as well as its contribution to improving wearing comfort.

## 4. Discussions

### 4.1 Validity of the Regression Model Derived under Static Conditions

In this study, the flow characteristics of the supply unit were modeled under static conditions, with the respiratory airflow simulator inactive. The supply flow rate was expressed as a function of differential pressure  $\Delta P$  and PWM duty value  $\mathbf{n}$ , and the resulting regression model  $Q_e(\Delta P, \mathbf{n})$  was derived. Furthermore, this regression model was applied under dynamic conditions to estimate flow rates. It was shown that even in a non-steady-state environment simulating respiratory activity, the simulated respiratory flow  $Q_3$  could be accurately reconstructed by subtracting the estimated supply flow rate  $Q_e(\Delta P, \mathbf{n})$  from the measured exhaust flow rate  $Q_2$ .

Notably, the transition from inhalation to exhalation - specifically the sign change in flow rate - was clearly reproduced by the estimated values derived from the regression model. This suggests the model's potential for use as a practical signal for detecting respiratory phases.

These results indicate that the regression model, constructed under steady-state conditions, can reasonably reflect the dynamic variations associated with actual breathing. This supports its fundamental applicability to real-time control systems.

However, the current experiments were conducted under fixed PWM duty value  $n$  and constant supply voltage  $V$ . For further development, it will be necessary to verify whether the instantaneous respiratory flow can still be accurately estimated when  $n$  is varied in real time in response to changes in respiratory flow (i.e., disturbance flow).

In such cases, it is expected that time delays and transfer function-like characteristics must be considered throughout the response process -from changes in  $n$ , to changes in fan speed, to changes in supply flow rate  $Q_1$ , and ultimately to changes in internal pressure  $\Delta P$ . Extending the model to account for these dynamic characteristics would improve the accuracy and reliability of respiratory flow estimation and assistive control under non-steady-state conditions.

#### 4.2 Limitations of the Experimental Setup and Future Improvements

The evaluation system developed in this study was originally designed as a foundational platform for quantitatively assessing the flow characteristics of the supply unit in a PAPR. However, its applicability extends beyond this primary function, and several potential extensions of its use are conceivable. In the following, we describe possible alternative configurations of the system as well as current limitations and directions for future improvements.

First, in what we refer to as the “nonwoven filter evaluation arrangement,” the supply unit in the current system can be replaced with a nonwoven fabric filter. This configuration allows for precise measurement of the differential pressure dependency of the airflow rate through the filter. Such a setup enables high-accuracy evaluation of the pressure loss characteristics of commercially available or newly developed nonwoven materials, making the system suitable for use as a filter performance evaluation platform.

Second, in the “PAPR simulation arrangement,” the exhaust tower connected to the system can be replaced with a nonwoven filter. In this configuration, air is supplied from the supply unit to the pressure buffer (which mimics the interior of a PAPR hood), and is then discharged through the nonwoven exhaust filter under positive pressure. When simulated respiratory flow is introduced by the respiratory airflow simulator, the resulting setup can reproduce the complete fluid dynamics of a PAPR system. This enables the construction and verification of a comprehensive fluid model of the PAPR, providing a valuable testing environment for the development of future control algorithms, including breathing-synchronized assistive control, leakage detection, and comfort evaluation.

On the other hand, the introduction of simulated breathing in the current setup is implemented manually using a piston-cylinder mechanism. Consequently, the reproducibility and quantitative accuracy of the inhalation/exhalation flow waveforms are limited. To obtain more precise and reproducible data, it will be necessary to introduce a linear actuator and implement program-controlled automation. This would allow the generation of realistic respiratory flow patterns (e.g., resting breathing, speech breathing, or exercise breathing) and significantly enhance the objectivity and versatility of the experiments.

In summary, the present evaluation system was designed not only for supply unit flow rate assessment, but also as a versatile platform for evaluating and simulating individual components and the overall system of a PAPR. With further expansion of the experimental environment and automation of the setup, more precise model development and real-time control testing are expected to become feasible in future studies.

#### 4.3 Practical Applications and Future Deployment Prospects

The flow rate regression model  $Q_e(\Delta P, n)$  developed in this study is highly implementable, as it enables estimation of respiratory states using only a small number of input parameters -namely, differential pressure  $\Delta P$  and PWM control signal  $n$ . This method allows for noninvasive and real-time detection of respiratory states (inhalation/exhalation), making it feasible to construct a PAPR that supports breathing through positive and negative pressure control based on the identified state.

Specifically, positive pressure within the hood can be increased during inhalation to assist airflow intake, while exhaust can be promoted during exhalation. Such a control mechanism is expected to reduce the user's respiratory burden. This functionality not only significantly improves wearing comfort for healthcare professionals and elderly individuals, but also lowers the barrier for long-term use among the general public.

Furthermore, the proven accuracy and stability of the regression model open the path to socially deploying a simplified yet intelligent PAPR system consisting only of a differential pressure sensor and control software. By integrating this pressure control model with algorithms for detecting pressure fluctuations associated with coughing or for identifying air leakage, potential applications could also extend to health monitoring and early detection of infection symptoms.

Looking ahead, this model could serve as the basis for the development of a smart PAPR that connects via Bluetooth to the user's smartphone, enabling the recording and management of wearing status and usage history. In such systems, individual usage data -such as wearing rate and respiratory load- could be encrypted and shared with healthcare institutions or administrative bodies, when necessary, thus facilitating public health responses to airborne infectious diseases [7,10,14,15].

In summary, the model and system proposed in this study are not merely technical developments but constitute a foundational step toward enhancing the social acceptance of PAPRs and expanding their feasibility as a key technology for airborne infection control.

## 5. Conclusions

In this study, an experimental system was developed to quantitatively evaluate the flow characteristics of the supply unit used in Powered Air-Purifying Respirators (PAPRs), and its validity was verified. The constructed system includes a pressure buffer and a respiratory airflow simulator, and is capable of accurately evaluating the dependency of the supply flow rate on differential pressure  $\Delta P$ , PWM duty value  $n$ , and supply voltage  $V$ .

Based on measurement data obtained under static conditions, a polynomial regression model was established to express the supply flow rate  $Q$  as a function of  $\Delta P$  and  $n$ . Furthermore, under dynamic conditions in which simulated respiratory flow  $Q_3$  was introduced, a method was proposed to reconstruct  $Q_3$  from the difference between the measured exhaust flow rate  $Q_2$  and the estimated supply flow rate  $Q_e$  derived from the regression model, and its validity was experimentally confirmed. These results indicate the potential for real-time estimation of respiratory states (inhalation/exhalation) based on differential pressure and control signals, and represent an important step toward the implementation of assistive control functionality and improved wearing comfort in PAPRs.

Moreover, the developed system is not limited to evaluating supply unit characteristics but also possesses the flexibility to be applied to the evaluation of airflow through nonwoven filters and the simulation of entire PAPR fluid systems. It thus holds potential as a development and testing platform for future breathing-synchronized control algorithms and smart PAPR systems.

Future work will include the validation of estimation accuracy under dynamic conditions with real-time changes in PWM control, automation of respiratory simulation using linear actuators, and the integration of visualization and recording functions for wearing status via Bluetooth. These efforts aim to advance the realization of next-generation PAPR systems suitable for social implementation.

## Funding

This research is funded by Japan Society for the Promotion of Science, Promotion of Joint International Research, KAKENHI (Grants-in-Aid for Scientific Research for FY2025, Issue No. 25KK00735).

## References

- [1] A. M. Tilstra, A. Polizzi, S. Wagner, et al., "Projecting the long-term effects of the COVID-19 pandemic on U.S. population structure," *Nat. Commun.*, vol. 15, no. 2409, 2024.  
<https://doi.org/10.1038/s41467-024-46582-4>

- [2] J. Gao, Y. Yin, K. R. Myers, et al., "Potentially long-lasting effects of the pandemic on scientists," *Nat. Commun.*, vol. 12, no. 6188, 2021.  
<https://doi.org/10.1038/s41467-021-26428-z>
- [3] J. T. Rothwell, A. Cojocaru, R. Srinivasan, et al., "Global evidence on the economic effects of disease suppression during COVID-19," *Humanities and Social Sciences Communications*, vol. 11, no. 78, 2024.  
<https://doi.org/10.1057/s41599-023-02571-4>
- [4] W. T. Harvey, A. M. Carabelli, B. Jackson, et al., "SARS-CoV-2 variants, spike mutations and immune escape," *Nat. Rev. Microbiol.*, vol. 19, pp. 409–424, 2021.  
<https://doi.org/10.1038/s41579-021-00573-0>
- [5] B. Nogrady, "WHO redefines airborne transmission: what does that mean for future pandemics?," *Nature*, 2024.  
<https://www.nature.com/articles/d41586-024-01173-7>
- [6] S. Kharroubi and F. Sale, "Are lockdown measures effective against COVID-19?," *Front. Public Health*, vol. 8, 549692, 2020.  
<https://doi.org/10.3389/fpubh.2020.549692>
- [7] Y. Fujii, "An Engineering Alternative to Lockdown During COVID-19 and Other Airborne Infectious Disease Pandemics: Feasibility Study", *JMIR Biomedical Engineering*, vol.9, 2024.  
<https://biomedeng.jmir.org/2024/1/e54666>
- [8] Occupational Safety and Health Administration (OSHA), "Assigned protection factors for the revised respiratory protection standard," OSHA 3352-02, 2009.  
<https://www.osha.gov/sites/default/files/publications/3352-APF-respirators.pdf> [Accessed: Feb. 19, 2025].
- [9] Occupational Safety and Health Administration (OSHA), "Personal protective equipment," OSHA 1910.134.  
<https://www.osha.gov/laws-regs/regulations/standardnumber/1910/1910.134> [Accessed: Feb. 19, 2025].
- [10] Y. Fujii, "Examination of the requirements for powered air-purifying respirator (PAPR) utilization as an alternative to lockdown", *Scientific Reports*, vol.15, 1217, 2025.  
<https://www.nature.com/articles/s41598-024-82348-0>
- [11] R. M. Galindo, A. Takita, E. Carcasona, E. Magalang, T. S. Galindo, S. Hashimoto, T. Yamaguchi, E. U. Tibay, D. W. Shu, H. Kobayashi, K. Amagai, N. Ohta, N. Yoshiura, A. Kuwana, A. Yano and Y. Fujii, "Low-Cost Powered Air-Purifying Respirator (PAPR) "Distancing-Free Mask Frontline (DFM-F) Prototype No.1" for the Operational Tests in Hospitals in Cebu City, Philippines", *Journal of Mechanical and Electrical Intelligent System*, vol.5, no.2, pp.1-6, 2022.  
[http://jmeis.e-jikei.org/ARCHIVES/v05n02/JMEIS\\_v05n02a001.pdf](http://jmeis.e-jikei.org/ARCHIVES/v05n02/JMEIS_v05n02a001.pdf)
- [12] E. Carcasona, R. M. Galindo, A. Takita, E. Magalang, T. S. Galindo, S. Hashimoto, T. Yamaguchi, E. U. Tibay, D. W. Shu, H. Kobayashi, K. Amagai, N. Ohta, N. Yoshiura, A. Kuwana, A. Yano and Y. Fujii, "Very-Low-Cost Powered Air-Purifying Respirator (PAPR) "Distancing-Free Mask Industry

(DFM-I) Prototype No.1” and Proposal for a Lockdown-Free Industry”, *Journal of Technology and Social Science*, Vol.6, No.2, pp.1-4, 2022.

[http://jtss.e-jikei.org/issue/archives/v06n02/JTSS\\_v06n02a001.pdf](http://jtss.e-jikei.org/issue/archives/v06n02/JTSS_v06n02a001.pdf)

[13] A. Iizuka, R. M. Galindo, E. Carcasona, A. Takita and Y. Fujii, “Evaluation of Air-supply Units of Powered Air-Purifying Respirators”, *Proceedings of International Conference on Technology and Social Science 2024 (ICTSS 2024)*, I-01-02, (Online & Onsite Cebu, Philippines) December 2024.

[https://conf.e-jikei.org/ICTSS/2024/proceedings/materials/proc\\_files/IPS01/ICTSS2024\\_IPS01\\_02.pdf](https://conf.e-jikei.org/ICTSS/2024/proceedings/materials/proc_files/IPS01/ICTSS2024_IPS01_02.pdf)

[14] Y. Fujii, A. Takita, T. Yamaguchi and S. Hashimoto, Japanese Patent, no.7616624. (Patented on 8 January 2025).

[https://jglobal.jst.go.jp/detail?JGLOBAL\\_ID=202503001572519658](https://jglobal.jst.go.jp/detail?JGLOBAL_ID=202503001572519658)

[15] Y. Fujii, A. Takita and S. Hashimoto, Japanese Patent, no.7515044. (Patented on 4 July 2024).

[https://jglobal.jst.go.jp/detail?JGLOBAL\\_ID=202403002056869269](https://jglobal.jst.go.jp/detail?JGLOBAL_ID=202403002056869269)